JOURNAL OF AIRCRAFT
Vol. 29, No. 5, Sept.–Oct. 1992

High Angle-of-Attack Flush Airdata Sensing System

Stephen A. Whitmore* and Timothy R. Moes†
NASA Ames Research Center, Edwards, California 93523
and
Terry J. Larson‡
PRC Systems, Inc., Edwards, California 93523

A nonintrusive high angle-of-attack flush airdata sensing system (HI-FADS) was installed and flight tested on the F-18 high alpha research flight vehicle (HARV). This system measures airdata using a matrix of 25 flush-pressure orifices on the vehicle nose. Satisfactory results were obtained using all 25 ports and a symmetric subset of just 9 ports. The overall HI-FADS system design and development including hardware, air-data algorithm, and system calibration is presented. Flight test validation results are presented. Under moderate maneuvering conditions the system is shown to give excellent results.

Nomenclature

A = first aerodynamic model coefficient
B = second aerodynamic model coefficient
C = linearized observation matrix
C_p = pressure coefficient
$F[\ldots]$ = aerodynamic model functional
i = port index
j = iteration index
M_∞ = freestream Mach number
N = total number of pressure obervations
P_∞ = freestream static pressure, lbf/ft^2, kPa
p = surface pressure, lbf/ft^2, kPa
Q = least squares weighting function
$\bar{q}_\infty$ = freestream incompressible dynamic pressure, lbf/ft^2, kPa
q_{c_∞} = freestream compressible dynamic pressure, lbf/ft^2, kPa
$\boldsymbol{R}$ = surface position vector, ft, m
$\boldsymbol{V}$ = velocity vector, ft/sec, m/s
$\boldsymbol{X}$ = state vector
$\boldsymbol{Z}$ = observation vector
α = generic angle-of-attack symbol, deg
α_e = effective angle-of-attack, deg
α_∞ = freestream angle-of-attack, deg
β = generic angle-of-sideslip symbol, deg
β_e = effective angle-of-sideslip, deg
β_∞ = freestream angle-of-sideslip, deg
$\delta\alpha$ = angle-of-attack calibration parameter, $\alpha_e - \alpha_\infty$, deg
$\delta\beta$ = angle-of-sideslip calibration parameter, $\beta_e - \beta_\infty$, deg
$\delta\boldsymbol{X}$ = state vector iteration error
$\delta\boldsymbol{Z}$ = model prediction iteration factor
ε = HI-FADS model calibration factor
θ = flow incidence angle, deg
λ = normal angle coordinate, deg
ϕ = clock angle coordinate, deg

Presented as Paper 90-0232 at the AIAA 28th Aerospace Sciences Meeting, Reno, NV, Jan. 8–11, 1990; received Dec. 31, 1990; revision received Nov. 9, 1991; accepted for publication Nov. 9, 1991.

*Senior Aerospace Engineer, Dryden Flight Research Facility, Fluid and Flight Mechanics Branch, P.O. Box 273. Member AIAA.
†Aerospace Engineer, Dryden Flight Research Facility, Fluid and Flight Mechanics Branch, P.O. Box 273. Member AIAA.
‡Analyst, Aerodynamics Support Group, P.O. Box 273. Member AIAA.

Introduction

AT high angles-of-attack where aircraft stall is imminent and small changes in angle-of-attack can greatly influence aerodynamic properties of the aircraft, the problem of flight control augmentation is extremely complicated. In this flight regime, it is critical that accurate measurements of airdata parameters including angle-of-attack, angle-of-sideslip, Mach number, and dynamic pressure be available for use by the flight augmentation system. Unfortunately, at high angles-of-attack it is difficult to accurately measure airdata using traditional intrusive sensing devices such as probes or nose-booms. Intrusive flow measurements on the aircraft nose alter the basic flow characteristics around the nose and affect both stall onset and poststall performance characteristics.[1,2] Because of the large influences of upstream vortices and flow separations at high angles-of-attack, off-nose measurement locations are unsatisfactory.

The HARV flight test program, whose principle objective was to study aerodynamics at high angle-of-attack, required accurate airdata estimates throughout the entire subsonic flight envelope, especially at high angles-of-attack. In order to accurately characterize the high angle-of-attack aerodynamics of the vehicle, it was determined that the airdata measurements should be obtained nonintrusively. As a means of circumventing this difficulty, a nonintrusive HI-FADS was installed and flight tested on the HARV.

The HI-FADS system design is an evolution from prototype nonintrusive airdata systems flight tested on the KC-135 and F-14 vehicles. These systems were intended only to demonstrate the feasibility of the concept, and did not attempt to derive algorithms capable of operating as a fully redundant flight measurement system.[3,4] The emphasis of these earlier programs was the measurement and presentation of individual pressure coefficient data and their empirical relationships to the airdata parameters. This HI-FADS system, whose results are to be presented in this paper, emphasises the overall design for high angle-of-attack with particular attention directed towards airdata algorithm development and system calibration. Composite results are expressed as airdata estimates instead of raw pressure values.

Aircraft Measurement Aquisition System

For the HARV flight tests a special research measurement acquisition system was installed. Research system measure-

ments included: linear accelerations from a set of body-axis accelerometers; three-axis angular velocities from a body-axis rate-gyro package, airdata from two calibrated wingtip airdata booms, and pressure data from the HI-FADS system. In addition to these measurements velocity, aircraft attitudes, and altitude from the aircraft inertial navigation system (INS) were also interfaced with the research measurement acquisition system. All data were digitally encoded onboard using 10-bit pulse code modulation (PCM) and telemetered to ground where they were displayed in real time and recorded for postflight analysis.

The flight test noseboom was removed to make way for the HI-FADS installation. The wingtip sidewinder launch racks were removed and replaced with special camera pods and wingtip airdata booms. The right wingtip airdata boom consisted of a standard NACA pitot-static head with flow direction vanes.[5-7] The left wingtip airdata boom consisted of a specially constructed swivel-head designed to align with the local air-velocity vector. This swivel design effectively eliminated total pressure loss at all angles-of-attack. Flow direction sensing vanes were also installed on the left wingtip boom. Both wingtip booms were calibrated to a steady-state accuracy of better than ± 0.005 in Mach number and ± 0.5 deg in angle-of-attack and sideslip. Calibration validity range for the wingtip airdata sensors extended up to 40.0 deg angle-of-attack. Beyond 40 deg angle-of-attack the accuracy of the wingtip sensor measurements diminished rapidly. Specific details concerning the wingtip sensor hardware, installation, and calibration are presented in Refs. 8 and 9. The wingtips flexed dramatically and nonlinearly under loaded or dynamic conditions, dynamic accuracy estimates for the wingtip booms are unavailable.

The HI-FADS configuration has a simple hardware arrangement with the basic fixture being a small fiberglass reinforced plastic nosecap. A set of 25, 0.06 in. diam pressure orifices, arranged in annular rings, were drilled in the nosecap. Flight tests were conducted using a 25-port arrangement with ports arranged in four rings and a single nosetip port. The rings were distributed in a symmmetric radial pattern about the nosecap axis of symmetry. Analyses were performed using all 25 orifices and a subset of 9 orifices. The locations of the nosecap ports were determined using a normal and clock angle coordinate system measured relative to the axis of symmetry. The normal angle, λ, is defined as the angle that the gradient to the surface makes with respect to the nosecap axis of symmetry. The clock angle, ϕ, is defined as the angle, looking aft, around the axis of symmetry, measured in a clockwise sense starting at the aircraft Z-axis (bottom of aircraft). Figure 1 illustrates the definitions of the normal and clock coordinate angles and the locations of the pressure ports on the aircraft nose.

Pressures at the nosecap were sensed by a multiple transducer, electronically scanned pressure (ESP) module, remotely mounted in the aircraft nose cavity. Pressures were transported to the ESP module using lengths of flexible pneumatic tubing. Analyses performed in Ref. 10 indicate that the pneumatic tubing did not introduce any significant distortions in the measured pressure values in the bandwith of interest (0–20 Hz).

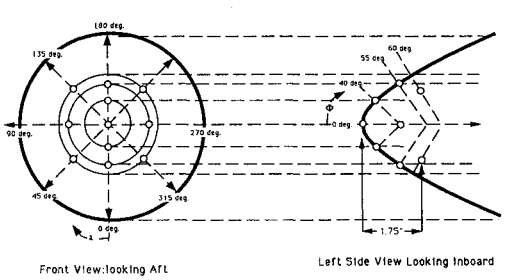

Fig. 1 Schematic of HI-FADS nosecap showing coordinate definitions and port locations.

Flow Analysis and Pressure Modeling

This section presents the aerodynamic model used to relate the HI-FADS pressure measurements to the desired airdata quantities. Using the developed model, all available pressure measurements can be used simultaneously to estimate the complete airdata state using nonlinear regression. The use of an overdetermined (more observations than states) analysis makes the resulting algorithm robust to small perturbations in the measured pressure data.

Reference 11 develops the aerodynamic model for the HI-FADS system in detail. The model developed from potential flow for a source in uniform flow, expresses the surface pressure coefficient in terms of the flow incidence, θ as

$$C_p(\theta) = \frac{q_c}{q}\left[\cos^2(\theta) + \varepsilon \sin^2(\theta)\right]$$

To account for nonideal nose shape, compressibility, and afterbody effects, the parameter ε is allowed to vary smoothy as a function of flight conditions throughout the Mach number range, and eventually ε tapers to zero at very high speeds. With ε set to zero, the pressure coefficient model is simply modified Newtonian flow on a hemisphere, thus the pressure model can be calibrated for application to flows ranging from subsonic to hypersonic conditions.

The incidence angle may be written in terms of angle-of-attack and angle-of-sideslip by taking the inner product of the position vector with the velocity vector

$$\cos(\theta) = \frac{\boldsymbol{V}\cdot\boldsymbol{R}}{\|\boldsymbol{V}\|\,\|\boldsymbol{R}\|}$$

$$= \cos(\alpha)\cos(\beta)\cos(\lambda) + \sin(\beta)\sin(\phi)\sin(\lambda)$$

$$+ \sin(\alpha)\cos(\beta)\cos(\phi)\sin(\lambda)$$

Applying the definition to the pressure coefficient

$$C_p(\theta) = \frac{p_\theta - p_\infty}{\bar{q}}$$

the model reduces to

$$p_\theta = q_c[\cos^2(\theta) + \varepsilon \sin^2(\theta)] + p_\infty$$

Thus for a given location on the surface

$$p(\phi, \lambda) = F(\alpha, \beta, q_c, p_\infty, \phi, \lambda, \varepsilon)$$

where α, β, q_c, P_∞ are airdata parameters, ϕ, λ are orifice coordinate angles, and ε is a calibration parameter yet to be empirically determined.

The potential flow model assumes a nonlifting hemisphere with no trailing afterbody. Clearly, this is not the case for the nose of an aircraft where vehicle induced upwash and sidewash alter the local flow angles.[12] Thus the HI-FADS system measures local or effective (α_e, β_e) and not freestream (α_∞, β_∞) angles-of-attack and sideslip. Effective and freestream angles are related by

$$\alpha_e = \alpha_\infty + \delta\alpha$$

$$\beta_e = \beta_\infty + \delta\beta$$

where, $\delta\alpha$ and $\delta\beta$ are calibration factors that must also be empirically identified.

Calibration of HI-FADS System

The HI-FADS system was calibrated using reference airdata generated from flight data by means of the minimum variance estimation techniques of Refs. 13–16. In this pro-

cedure, high-accuracy, high-fidelity reference airdata are generated by merging complementary information from multiple data sources, provided by the research data acquisition system and external measurements, such as radar tracking and analyses of weather balloon information.

All flight maneuvers used to perform the calibration analyses were pre- and postceded by stabilized low-to-moderate angle-of-attack flight. During this stabilized flight, the wingtip boom airdata were weighted heavily to give initial and final estimates of the atmospheric winds. During the course of the calibration maneuvers, filter weights were adaptively varied to weight the wingboom airdata inversely proportional to both pitch-rate and angle-of-attack. At the same time, the equivalent time constant of the wind states was increased in direct proportion to pitch-rate and angle-of-attack. Weights on the inertial and meteorological data were held constant throughout the maneuver. Maneuver reference airdata were generated off-line and stored for later use in the calibration analyses.

A maneuver was judged to be good for calibration purposes when the resulting wind estimates showed little or no correlation to aircraft dependent velocity parameters. The basic premise of this technique is that atmospheric winds, although they may change during the course of a flight maneuver, should change independently of aircraft motions. Examination of filter covariance estimates, indicates that the resulting reference airdata estimates have a rms noise level of approximately 0.001 in Mach number, 0.1 deg in angle-of-attack and angle-of-sideslip, and 10 ft (3.05 m) in altitude.

The calibration parameters $\delta\alpha$, $\delta\beta$, and ε were estimated by substituting the reference airdata into the flow model and comparing the model pressure predictions to the pressures that were actually measured. Residuals between the measured and predicted pressures were used to infer the values of the calibration parameters at each data frame using nonlinear regression.

Calibration data were obtained for Mach numbers up to 1.20 and angles-of-attack up to 55.0 deg. Calibrations performed for both the 9-port and 25-port configurations were found to be nearly identical, thus it is concluded that the calibration is mostly influenced by the aircraft configuration (within reason) and not the individual port layout. Systematic trends were identified by plotting the estimated calibration parameters—the results of the regression—as a function of various flight variables and visually inspecting the results. Once trends were identified, a series of tabular breakpoints were derived using curve-fits, and the tables were hard-coded into the algorithm. The resulting calibration trends were presented in detail in Ref. 11.

HI-FADS Algorithm

This section derives the HI-FADS system matrix equations and the regression formulae used to solve the system. Assuming that an estimate of the jth freestream airdata state is available, if the calibrated flow model is expanded and linearized about this estimate

$$\begin{bmatrix} p_{1_{j+1}} - F_{1_{|j}} \\ p_{2_{j+1}} - F_{2_{|j}} \\ \cdots \\ p_{N_{j+1}} - F_{N_{|j}} \end{bmatrix} = \begin{bmatrix} \left(\frac{\partial F_1}{\partial \alpha}\right)_{|j} & \left(\frac{\partial F_1}{\partial \beta}\right)_{|j} & \left(\frac{\partial F_1}{\partial P_\infty}\right)_{|j} & \left(\frac{\partial F_1}{\partial q_{c_\infty}}\right)_{|j} \\ \left(\frac{\partial F_2}{\partial \alpha}\right)_{|j} & \left(\frac{\partial F_2}{\partial \beta}\right)_{|j} & \left(\frac{\partial F_2}{\partial P_\infty}\right)_{|j} & \left(\frac{\partial F_2}{\partial q_{c_\infty}}\right)_{|j} \\ \cdots & \cdots & \cdots & \cdots \\ \left(\frac{\partial F_N}{\partial \alpha}\right)_{|j} & \left(\frac{\partial F_N}{\partial \beta}\right)_{|j} & \left(\frac{\partial F_N}{\partial P_\infty}\right)_{|j} & \left(\frac{\partial F_N}{\partial q_{c_\infty}}\right)_{|j} \end{bmatrix} \cdot \begin{bmatrix} \alpha_{\infty_{j+1}} - \alpha_{\infty_j} \\ \beta_{\infty_{j+1}} - \beta_{\infty_j} \\ P_{\infty_{j+1}} - P_{\infty_j} \\ q_{c_{\infty_{j+1}}} - q_{c_{\infty_j}} \end{bmatrix} \tag{1}$$

where

$$F_{i_{|j}} = F\left\{\begin{bmatrix} \alpha_{\infty_j} \\ \beta_{\infty_j} \\ P_{\infty_j} \\ q_{c_{\infty_j}} \end{bmatrix}, \begin{bmatrix} \delta\alpha \\ \delta\beta \\ \varepsilon \end{bmatrix}, \begin{bmatrix} \phi_i \\ \lambda_i \end{bmatrix}\right\}$$

The parameters, $\delta\alpha$, $\delta\beta$, and ε, are computed using the previously determined calibration tables. If the left side of Eq. (1) is evaluated using measured pressure data, the N by 4 overdetermined linear system may be written in matrix form as

$$\delta Z = C\delta X + \text{error}$$

and solved using weighted iterative least squares[17]

$$\hat{X}_{j+1} = \hat{X}_j + [(C^T Q_{j+1} C)^{-1}] C^T Q_{j+1} [Z_{j+1} - \hat{Z}_j],$$

with

$$Z_{j+1} = \begin{bmatrix} p_{1_{j+1}} \\ p_{2_{j+1}} \\ \cdots \\ p_{N_{j+1}} \end{bmatrix}, \qquad \hat{Z}_j = \begin{bmatrix} \hat{F}_{1|j} \\ \hat{F}_{2|j} \\ \cdots \\ \hat{F}_{N|j} \end{bmatrix}$$

$$\hat{X}_{j+1} = \begin{bmatrix} \hat{\alpha}_{\infty_{j+1}} \\ \hat{\beta}_{\infty_{j+1}} \\ \hat{P}_{\infty_{j+1}} \\ \hat{q}_{c_{\infty_{j+1}}} \end{bmatrix}, \qquad \hat{X}_j = \begin{bmatrix} \hat{\alpha}_{\infty_j} \\ \hat{\beta}_{\infty_j} \\ \hat{P}_{\infty_j} \\ \hat{q}_{c_{\infty_j}} \end{bmatrix}$$

Here, Q is the weighting matrix for this iteration.

Within each frame, the algorithm is linearized about a starting value, the least squares state perturbations are computed, and the algorithm is iterated until convergence. At the beginning of each new data frame, the system is relinearized about the result of the previous frame and the iteration is repeated, thus, the algorithm is time-recursive as well as iterative. This recursive, iterative, and overdetermined structure (more observations than states) makes the algorithm stable and robust to perturbations in the measured pressure data. For the initial data frame, the algorithm is initialized about an arbitrary user-input starting value. More sophisticated startup techniques are currently being investigated.

Evaluation of HI-FADS System Performance

The performance of the HI-FADS system was empirically evaluated using flight data, where comparisons between various HI-FADS derived airdata estimates and the corresponding reference airdata parameters were performed. The reference airdata were generated using the same minimum variance estimation techniques as described previously. As an illustration of typical flight results, data from a moderate rate Dutch-roll maneuver will now be presented. These HI-FADS data, obtained using the 9-port analysis, were not previously used in establishing the calibration tables.

Comparisons of HI-FADS and reference angles-of-attack were presented in Fig. 2. Presented in Fig. 2a are the actual angle-of-attack time histories. Two curves are presented 1) the reference angle-of-attack and 2) the HI-FADS angle-of-attack. For the scale used, no differences are discernable. Actual differences may be discerned by plotting the time history of the residual between the HI-FADS and reference angles-of-attack. This residual time history is presented in Fig. 2b. Similar comparisons for Mach number are presented in Figs. 3a and 3b. With the exception of small deviations during the high-rate portions of the maneuver, the differences between the HI-FADS and reference airdata values are insignificant.

Table 1 HARV HI-FADS airdata residual statistics for 9-port and 25-port configurations

Parameter	Mean error 9-port	RMS error 9-port	Mean error 25-port	RMS error 25-port
Angle-of-attack	0.02 deg	0.56 deg	0.02 deg	0.48 deg
Angle-of-sideslip	0.10 deg	0.52 deg	0.10 deg	0.46 deg
Mach number	0.0008	0.004	0.0007	0.003
Altitude	11.4 ft (3.47 m)	19.2 ft (5.85 m)	9.2 ft (2.80 m)	16.3 ft (4.97 m)
Airspeed	0.84 ft/s (0.259 m/s)	4.0 ft/s (1.22 m/s)	0.75 ft/s (0.223 m/s)	3.0 ft/s (0.914 m/s)

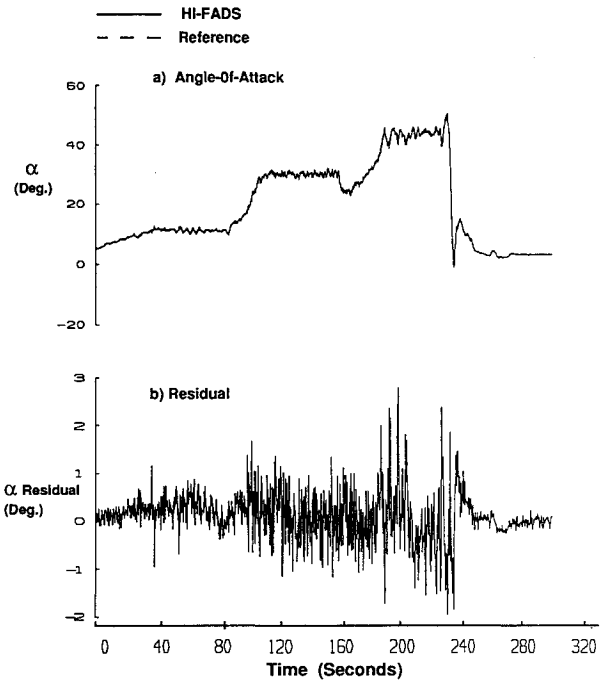

Fig. 2 Dutch-roll maneuver time history comparisons: angle-of-attack.

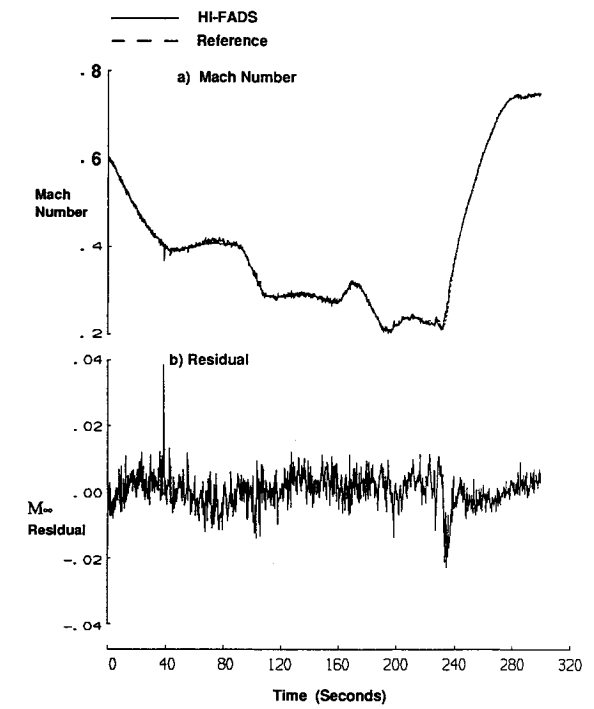

Fig. 3 Dutch-roll maneuver time history comparisons: Mach number.

Quantitative accuracy levels were obtained by evaluating residual statistics for a compilation of various HI-FADS maneuvers. These results are presented in Table 1 for both the 9-port and the 25-port analyses. HI-FADS airdata estimates resulting from 25-port analyses were slightly less noisy than for the 9-port analyses. Since the 25-port configuration is more overdetermined and thus less sensitive to individual measurement errors, this result is as expected. The statistical data indicate that even up to high angles-of-attack, both the 9-port and 25-port configurations have a standard deviation of approximately one-half in angle-of-attack and angle-of-sideslip, and better than 0.004 in Mach number. On a steady-state basis, the extremely low mean residual values indicate that the HI-FADS system can be calibrated as accurately as the reference against which it is being compared.

Under moderate maneuvering conditions, all flight data examined show that the HI-FADS system, both the 9-port and 25-port configurations, performs well over the entire subsonic and transonic Mach number ranges and up to 55 deg angle-of-attack. During heavy maneuvering (angular rates greater than 20 deg/s), aerodynamic lags in the aircraft flowfield, as well as the recursive nature of the algorithm, cause some minor performance degradation.

Results presented in Refs. 10 and 11 indicate that the frequency response of the system appears to be good to approximately 10 Hz. For a higher fidelity measurement, hybrid techniques that blend inertially derived information with the airdata measurements, may be required.[16] The frequency response capability must be studied further to determine the operational limits of the HI-FADS system.

Summary and Concluding Remarks

A prototype nonintrusive airdata system was installed and flight-tested at high angles-of-attack on the HARV. This system hardware consisted of a matrix of 25 pressure orifices arranged in concentric circles on the nose of the vehicle. The system was tested using all 25 pressure ports and a subset of 9 pressure ports. Pressure was transmitted from the orifices to a multiport electronically-scanned pressure module by way of lines of flexible pneumatic tubing. Outputs were digitized and telemetered to ground where they were recorded on tape for post-flight processing.

HI-FADS pressure measurements were related to the desired airdata quantities using a nonlinear aerodynamic model and all available pressure measurements were used simultaneously to estimate the complete airdata state. Within each data frame, the algorithm is linearized about a starting value, least squares state perturbations are computed, and the algorithm is iterated until convergence. At the beginning of each new data frame, the system is relinearized about the result of the previous frame, and the iteration is repeated, thus the algorithm is time-recursive as well as iterative. The recursive, iterative, and overdetermined structure (more observations than states) makes the algorithm stable and robust to perturbations in the measured pressure data. For the initial data frame, the algorithm is initialized about an arbitrary user-input starting value.

The HI-FADS system was calibrated and demonstrated using reference airdata generated by means of minimum vari-

ance estimation techniques that blended airdata measurements from two wingtip airdata booms with inertial velocities, aircraft angular rates and attitudes, precision radar tracking, and meteorological analyses. Flight test validation results demonstrate that under moderate maneuvering conditions the system gives excellent results. Empirical verification was performed over a large portion of the HARV flight envelope with a Mach number range of 0.15–1.20 and an angle-of-attack range from −8.0 to 55.0 deg.

Quantitative accuracy levels were obtained by evaluating residual (HI-FADS minus reference) statistics for HI-FADS flight maneuvers. Results are presented for both the 9-port and the 25-port analyses. Statistical data indicate that even up to high angles-of-attack, both the 9-port and 25-port configurations have a standard deviation of approximately one-half degree in angle-of-attack and angle-of-sideslip, and better than 0.004 in Mach number. These accuracy levels are equivalent to those of conventional intrusive airdata systems, but over a much wider angle-of-attack range. Analyses of residual mean values indicate that for steady-state conditions, the HI-FADS system can be calibrated as accurately as the reference against which it is being compared.

References

[1]Schneider, E. T., and Meyer, R. R., Jr., "F-18 High Alpha Research Vehicle Description, Results, and Plans," Society of Experimental Test Pilots, 1989 Rept. to the Aerospace Profession, Proceedings, San Diego, CA, 1989.

[2]Fisher, D. F., Del Frate, J. H., and Richwine, D. M., "In-Flight Flow Visualization Characteristics of the NASA F-18 HARV Aircraft at High Angles-of-Attack," Society of Automotive Engineers Paper 89-2222, Anaheim, CA, Sept. 1989.

[3]Larson, T. J., Whitmore, S. A., Ehernberger, L. J., Johnson, J. B., and Siemers, P. M., III. "Qualitative Evaluation of a Flush Air Data System at Transonic Speeds and High Angles of Attack," NASA TP 2716, April 1987.

[4]Larson, T. J., Whitmore, and Siemers, P. M., III, "Subsonic Investigation of an All Flush Orifices Airdata System," NASA TP-1643, May 1980.

[5]Gracey, W., "Wind-Tunnel Investigation of a Number of Total-Pressure Tubes at High Angles of Attack: Subsonic, Transonic, and Supersonic Speeds," NACA TR 1303, Hampton, VA, Jan. 1956.

[6]Gracey, W., "Measurement of Aircraft Speed and Altitude," NASA RP 1046, Hampton, VA, May 1980.

[7]Richardson, N. R., and Pearson, A. R., "Wind Tunnel Calibrations of A Combined Pitot-Static Tube, Vane-Type Flow-Direction Transmitter, and Stagnation-Temperature Element at Mach Numbers from 0.60 to 2.87," NASA TN-D122, Hampton, VA, Oct. 1959.

[8]Moes, T. R., and Whitmore, S. A., "A Preliminary Look at Techniques Used to Obtain Airdata From Flight at High Angles-of-Attack," NASA TN-101729, Edwards, CA, Dec. 1990.

[9]Geenan, R. J., Moulton, B. J., and Haering, E. A., "A System for Testing Airdata Probes at High Angles of Attack Using A Ground Vehicle," AIAA Paper 91-0088, Reno, NV, Jan. 1991.

[10]Whitmore, S. A., and Moes, T. R., "The Effects of Pressure Sensor Acoustics on Airdata Derived From a High-Angle-of-Attack Flush Airdata Sensing (HI-FADS) System," AIAA Paper 91-0671, Reno, NV, Jan. 1991.

[11]Whitmore, S. A., Moes, T. R., and Larson, T. J., "Preliminary Results From a Subsonic High Angle-of-Attack Flush Airdata Sensing (HI-FADS) System: Design, Calibration, and Flight Test Evaluation," NASA TM-101713, 1990.

[12]Kuethe, A. M., and Chow, C.-Y., "Foundations of Aerodynamics: Bases of Aerodynamic Design," 3rd ed., Wiley, New York, 1976, pp. 75–91.

[13]Whitmore, S. A., "Reconstruction of the Shuttle Reentry Air Data Parameters Using a Linearized Kalman Filter," AIAA Paper 83-2097, Gatlinburg, TN, Aug. 1983.

[14]Whitmore, S. A., "Formulation and Implementation of A Non-Stationary Adaptive Estimation Algorithm with Applications for Air-Data Reconstruction," NASA TM 86727, May 1985.

[15]Whitmore, S. A., Larson, T. J., and Ehernberger, L. J., "Air Position-Error Calibration Using State Reconstruction Techniques," NASA TM 86029, Sept. 1984.

[16]Moes, T. R., and Whitmore, S. A., "Preliminary Results from an Airdata Enhancement Algorithm with Applications to High Angle-of-Attack Flight," AIAA Paper 91-0672, Reno, NV, Jan. 1991.

[17]Brogran, W. L., "Modern Control Theory," 1st ed., Quantum Publishers, New York, 1974, pp. 226–228.